

Article

## Helical Oligourea Foldamers As Powerful Hydrogen Bonding Catalysts for Enantioselective C-C Bond-Forming Reactions

Diane Bécart, Vincent Diemer, Arnaud Salaün, Mikel Oiarbide, Yella-Reddy Nelli, Brice Kauffmann, Lucile Fischer, Claudio Palomo, and Gilles Guichard

*J. Am. Chem. Soc.*, **Just Accepted Manuscript** • DOI: 10.1021/jacs.7b05802 • Publication Date (Web): 07 Aug 2017

Downloaded from <http://pubs.acs.org> on August 7, 2017

### Just Accepted

“Just Accepted” manuscripts have been peer-reviewed and accepted for publication. They are posted online prior to technical editing, formatting for publication and author proofing. The American Chemical Society provides “Just Accepted” as a free service to the research community to expedite the dissemination of scientific material as soon as possible after acceptance. “Just Accepted” manuscripts appear in full in PDF format accompanied by an HTML abstract. “Just Accepted” manuscripts have been fully peer reviewed, but should not be considered the official version of record. They are accessible to all readers and citable by the Digital Object Identifier (DOI®). “Just Accepted” is an optional service offered to authors. Therefore, the “Just Accepted” Web site may not include all articles that will be published in the journal. After a manuscript is technically edited and formatted, it will be removed from the “Just Accepted” Web site and published as an ASAP article. Note that technical editing may introduce minor changes to the manuscript text and/or graphics which could affect content, and all legal disclaimers and ethical guidelines that apply to the journal pertain. ACS cannot be held responsible for errors or consequences arising from the use of information contained in these “Just Accepted” manuscripts.

# Helical Oligourea Foldamers as Powerful Hydrogen Bonding Catalysts for Enantioselective C-C Bond-Forming Reactions

Diane Bécart,<sup>a,b</sup> Vincent Diemer,<sup>a,f</sup> Arnaud Salaün,<sup>a</sup> Mikel Oiarbide,<sup>b</sup> Yella Reddy Nelli,<sup>a</sup> Brice Kauffmann,<sup>c</sup> Lucile Fischer,<sup>a</sup> Claudio Palomo,<sup>b\*</sup> and Gilles Guichard<sup>a\*</sup>

<sup>a</sup> Univ. Bordeaux, CNRS, CBMN, UMR 5248, Institut Européen de Chimie et Biologie, 2 rue Robert Escarpit, F-33607 Pessac, France ; <sup>b</sup> Departamento de Química Orgánica I, Facultad de Químicas, Universidad del País Vasco UPV/EHU, Apdo. 1072, 20080 San Sebastián, Spain; <sup>c</sup> Univ. Bordeaux, CNRS, INSERM, UMS3033/US001, Institut Européen de Chimie et Biologie, F-33607 Pessac, France

**ABSTRACT:** Substantial progress has been made towards the development of metal-free catalysts of enantioselective transformations, yet the discovery of organic catalysts effective at low catalyst loadings remains a major challenge. Here we report a novel synergistic catalyst combination system consisting of a peptide-inspired chiral helical (thio)urea oligomer and a simple tertiary amine that is able to promote the Michael reaction between enolizable carbonyl compounds and nitroolefins with excellent enantio-selectivities at exceptionally low (1/10000) chiral catalyst/substrate molar ratios. In addition to high selectivity – which correlates strongly with helix folding – the system we report here is also highly amenable to optimization, as each of its components can be fine-tuned separately to increase reaction rates and/or selectivities. The predictability of the foldamer secondary structure coupled to the high-level of control over the primary sequence results in a system with significant potential for future catalyst design.

## INTRODUCTION

The ability to synthesize sequence-based non-natural oligomers that fold with high fidelity – foldamers – raises new prospects for mimicking biopolymers and for creating molecules with emergent functions tailored to various applications.<sup>1</sup> The structure-guided design of foldamers that specifically recognize the surfaces of target biomacromolecules<sup>2</sup> or interact with small molecular guests,<sup>3,4</sup> as well as the fabrication of large architectures consisting of multiple secondary structure elements arranged in tertiary and quaternary structures,<sup>5,6</sup> represent significant recent achievements in this direction. Bioinspired catalysis is another area in which foldamers have far-reaching potential, yet little progress has been made in this direction, despite the (theoretical) suitability of foldamers as biomimetic catalysts. For example, foldamer systems typically exhibit long-range conformational (e.g. helical) order, a property beyond the reach of small molecules and little explored in enantioselective catalysis.

Enzymes are generally regarded as highly efficient catalysts at low loading levels, and commonly act through a mechanism involving multiple cooperative interactions.<sup>7</sup> Likewise, pre-organization of multifunctional catalysts through folding would be

expected to contribute to enhanced catalysis efficiency through (i) cooperative substrate binding, (ii) specific stabilization of charged transition-states and intermediates and (iii) minimization of the entropic cost of transition-state binding.<sup>8</sup> Synthetic  $\alpha$ -peptides for example have received strong interest as bioinspired catalysts.<sup>9,10</sup> In general, the active site consists of an array of reactive side chains pre-organized in space through folding;<sup>9</sup> more rarely, it involves main-chain functional groups.<sup>11</sup> However – and in contrast to peptides which have gained a momentum as middle size catalysts for a number of stereoselective, regioselective and chemoselective transformations<sup>9-13</sup> – synthetic foldamers are yet to be fully explored as asymmetric catalysts.<sup>14-19</sup>

Chiral aliphatic N,N'-linked oligoureas<sup>20-23</sup> are robust helical foldamers bearing structural resemblance to the  $\alpha$ -helical peptide backbone. Oligoureas typically mediate molecular recognition events through arrays of side chains displayed at the helix surface,<sup>24-26</sup> yet the main chain itself is highly-suited to bind small guest molecules. In particular, urea NHs at the positive end of the oligourea helix macrodipole have been shown to readily bind anions.<sup>27,28</sup> The finding that anion binding occurs without helix unfolding suggested to us that

oligourea foldamers could be useful in hydrogen bond catalysis.<sup>29</sup>

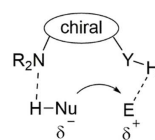
Herein, enantiopure helical oligo(thio)urea foldamers have been investigated for the first time in the context of enantioselective carbon-carbon bond forming reactions. We provide evidence that short helically folded aliphatic N,N'-linked oligoureas in combination with a simple achiral Brønsted base cocatalyst do work synergistically to promote the addition of carbonyl pronucleophiles to nitroalkenes with high reactivity and selectivity. A detailed structure-activity relationship study including a chain length dependence test<sup>30</sup> demonstrated the strong correlation between the folding propensity of the oligomer (a property beyond the reach of small molecule catalysts) and its catalytic performance.

## RESULTS AND DISCUSSION

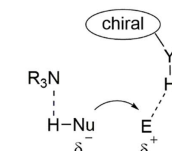
**Background, working hypothesis and design of helical oligo(thio)urea H-bond donor catalysts.** H-bond catalysis has become a major strategy for the activation of substrates in enantioselective organic reactions.<sup>31</sup> Among the suitable H-bond donor groups, (thio)ureas have shown to be highly effective and versatile, either as discrete catalyst or as integral part of a bifunctional Brønsted base-H-bond catalyst unit (Fig. 1a, left).<sup>29,31-40</sup> During the search of (thio)urea catalysts with improved activity and/or selectivity, the Smith laboratory discovered that thiourea catalysts featuring cooperative intramolecular H-bonds were more effective than simple thioureas in Mukaiyama-Mannich reaction models (Fig. 1b).<sup>8</sup> The Pihko group further refined this concept and reported the design of tertiary amine/bis(thio)urea bifunctional catalysts with improved activity in Mannich reactions of malonates and ketoesters with imines.<sup>37,40</sup> Also, Clayden has reported an internally organized bifunctional amine/thiourea catalyst that achieves remote asymmetric induction.<sup>19</sup> In addition to the benefits resulting from pre-organization of multifunctional catalysts through folding as noted above, it was suggested that the cooperative intramolecular H-bonding within the catalyst structure would (i) enhance the H-bond-donor ability of the thiourea group and (ii) liberate space around thiourea moiety for effective substrate-catalyst coordination. Based on these precedents, and inspired by the way enzymes engage large networks of cooperative intramolecular H-bonds, we hypothesized that chiral (thio)urea catalysts capable of forming extended intramolecular H-bonding networks – e.g. helical N,N'-linked oligoureas (Fig. 1c) – should present a unique catalytic profile.

### a Strategies for dual activation of nucleophile and electrophile

Bifunctional activation

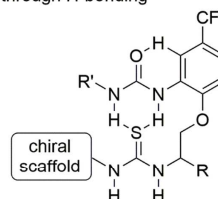


Synergistic activation



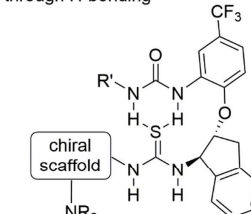
### b Improving the catalytic profile of thiourea catalysts

Chiral H-bond small molecule catalyst preorganized through H-bonding



(Smith, 2009)

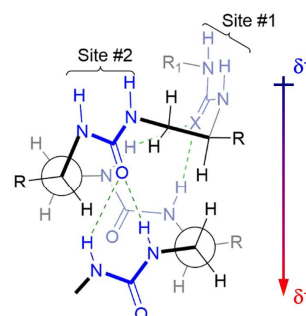
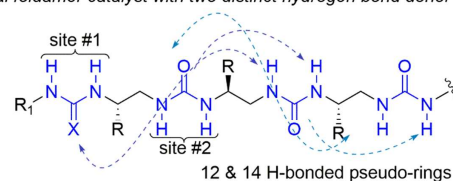
Bifunctional H-bond small molecule catalyst preorganized through H-bonding



(Pihko, 2012)

### c This work

Helical foldamer catalyst with two distinct hydrogen bond donor sites



- Preorganization based on folding
- Two distinct recognition sites (different pKa depending on R<sup>1</sup>)
- Controlled distance and orientation between sites #1 & #2
- Contribution of the helix macrodipole

**Figure 1.** Rationale for the use of Helical oligo(thio)urea foldamers as chiral components of binary catalytic systems. (a) Bifunctional and synergistic activation with H-bond donor catalysts;<sup>29,31-40</sup> (b) di-(thio)urea catalysts forming cooperative intramolecular H-bonds; (c) Representation of the extended chain of an N,N'-linked oligourea and its folded behavior<sup>22,27</sup> illustrating the two accessible H-bond donor sites near the positive pole of the helix macrodipole.

At the outset, we decided to validate this idea in the context of synergistic nucleophile/electrophile activation strategy<sup>41</sup> (Fig. 1a, right). Synergistic systems are highly modular and allow for an easier optimization

of each catalyst component separately. Our second assumption was that while a relatively high concentration of (achiral) base may be required for the activation of the C–H pronucleophile (to reach threshold concentration of the actual nucleophile), conversely relatively low amounts of the (chiral) H-bond donor catalyst might suffice if, during the subsequent C–C bond-forming (and stereochemistry-determining) step, a cooperative H-bond network with strong stereo-directing power operates.

In this work, we focused on 6-mer oligoureas which are known to adopt a well-defined helical conformation in both polar and non-polar solvents.<sup>27,42</sup> To differentiate the two sites available for substrate recognition and catalysis (Fig. 1c), we increased the polarity and the polarizability of the first urea group by introducing a 3,5-bis(trifluoromethyl)phenyl group (oligomer **1a**) and/or replacing the urea moiety by a thiourea (oligomer **2a**) moiety (Fig. 2). The primary structure (i.e. the sequence) of both oligomers is similar and consists of the repeat of three residues of (*S*)–

configuration with different proteinogenic side chains (Me, *i*Pr and *i*Bu) to enable an unambiguous assignment of all backbone protons.

Crystals suitable for X-ray diffraction of both oligomers **1a** and **2a** were obtained, and the structures solved by direct methods in the P<sub>2</sub><sub>1</sub> and P<sub>1</sub> space groups, respectively. The crystal structures of **1a** and **2a** (Fig. 2) which contain four and two independent molecules in the asymmetric units, respectively, (see Supplementary Fig. 1a,b) show that both oligomers have right-handed (*P*) helicity with both carbonyl and/or thiocarbonyl groups of the first two (thio)urea units engaged in intramolecular H-bonding. As expected,<sup>42</sup> the main differences between **1a** and **2a** resides in the geometry of the first intramolecular hydrogen bond between the terminal C=X and the NHs of the third urea group (the C=X...N distance increases from an average 2.90 Å in **1a** to 3.42 Å distance in **2a**) that leads to a slight rearrangement of the first residue and of the 3,5-bis(trifluoromethyl)phenyl moiety.

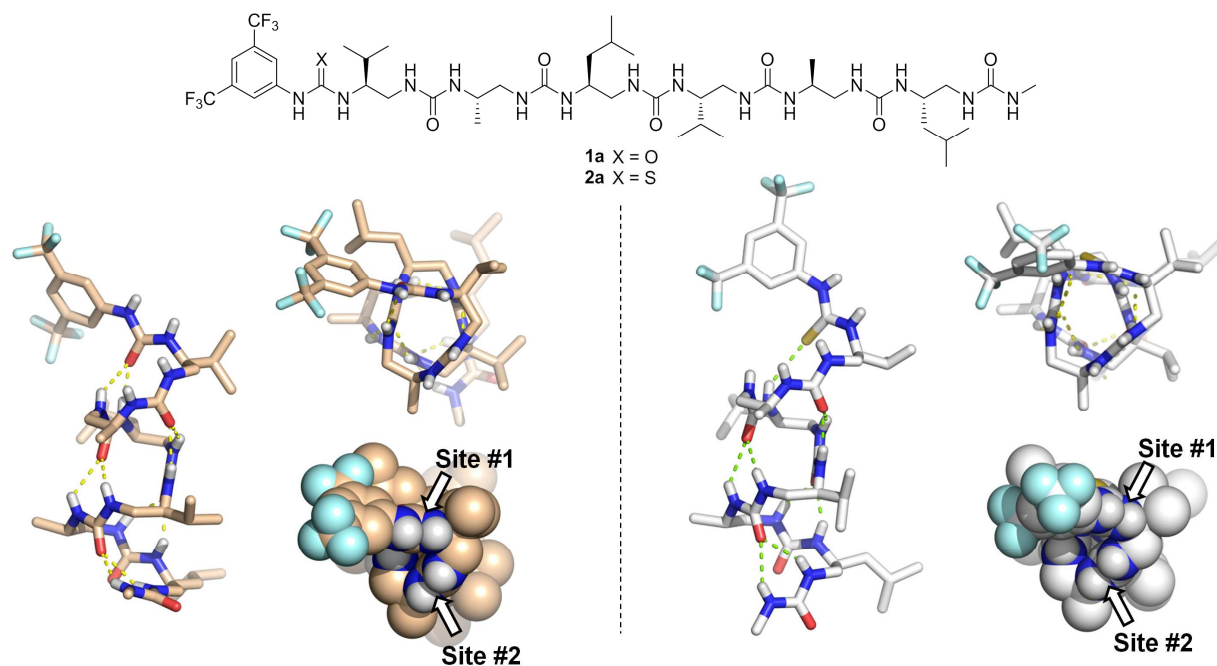


**Figure 2.** Foldamer-based chiral catalysts. Primary sequence of (thio)urea hexamers **1a** and **2a** and view along and down helical axis of their X-ray crystal structures showing accessibility of H-bond donor sites. The two helices are colored separately (**1a**, left and **2a**, right). The asymmetric units of **1a** and **2a** contain four and two independent molecules, respectively, of which only one is represented here (see supplementary Fig. S1 for a structural alignment of all independent molecules in the asymmetric unit).

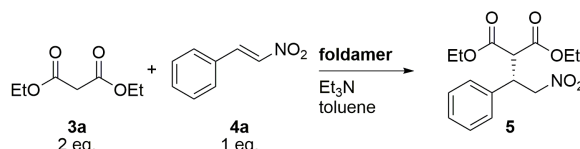
**A synergistic catalytic system at low chiral catalyst/substrate ratio.** The conjugate addition<sup>43</sup> of malonate ester (e.g. **3**) to nitroalkenes (e.g. **4**),<sup>44</sup> was selected to assess the viability of the approach. This reaction is synthetically interesting due in part to the rich chemistry of the nitro group,<sup>45</sup> and also because the

resultant  $\gamma$ -nitro carbonyl adducts can be easily transformed into  $\gamma$ -amino acids,  $\gamma$ -butyrolactams and pyrrolidines, all of which are interesting building blocks for pharmaceutical developments.<sup>46</sup> Initial catalytic activities (addition of diethyl malonate **3a** to nitrostyrene **4a**) were measured at different

concentrations (from 1 to 0.00025 mol%) of **1a** (or **2a**) in non-polar solvents in the presence of a fixed amount of Brønsted base (Et<sub>3</sub>N, 10 mol%). Several interesting trends were observed from this first series of experiments (Table 1, entries 1-13, Supplementary Table 1 and Supplementary Fig. 2a).

The combination of **1a** (0.1 mol%) and Et<sub>3</sub>N (10 mol%) in toluene at -20 °C was found to provide complete conversion and excellent enantioselectivities (95% ee<sup>47</sup>), thus denoting that separate Brønsted base and chiral H-bond donor work synergistically (Table 1, entry 2 and Supplementary Table 1, entry 1).<sup>48</sup> There was almost no conversion in the absence of **1a** (Et<sub>3</sub>N alone, entry 1).

**Table 1. Optimization of the foldamer/base catalytic system and structure-activity relationship study.**



Entry	Chiral Catalyst	Foldamer Loading (mol%)	Temperature (°C)	Reaction Time (h)	Et <sub>3</sub> N (mol%)	Conversion (%)	Yield (%)	ee (%)
1	-	-	-20	48	10	7	n.d.	0
2	<b>1a</b>	0.1	-20	48 (24)	10	100 (99)	86 (63)	95 (94)
3	<b>1a</b>	0.05	-20	48	10	100	85	94
4	<b>1a</b>	0.01	-20	48	10	98	82	91
5	<b>1a</b>	0.005	-20	48	10	93	82	84
6	<b>1a</b>	0.001	-20	48	10	67	49	74
7	<b>1a</b>	0.1	-20	48	1	56	43	95
8	<b>1a</b>	0.1	-20	48	5	100	85	95
9	<b>1a</b>	0.1	-20	48	20	100	83	93
10	<b>1a</b>	0.1	-20	16	30	100	78	93
11	<b>1a</b>	0.1	RT	48	10	98	75	89
12	<b>2a</b>	0.1	-20	48 (24)	10	98 (94)	80 (59)	93 (88)
13	<b>2a</b>	0.1	RT	48	10	94	74	86

Reactions were performed with 0.5 mmol of **4a** and 1.0 mmol of **3a**. Yields correspond to isolated compound after chromatographic purification. The enantiomeric excess (*ee*) was determined by chiral HPLC analysis. Absolute configuration (*R*) or (*S*) was known or assigned by analogy.

Remarkably, the reactivity and the selectivity of the catalytic system (**1a**/Et<sub>3</sub>N) remained largely unaffected when the chiral catalyst/substrate ratio was decreased to levels as low as 1:10000 (Table 1, entries 2-4 and Supplementary Fig. 2a). When as little as 0.01 mol% of **1a** was employed, the Michael adduct **5** was still obtained in a yield of 82% with 91% *ee* (Table 1, entry 4). Note that just 0.05 mg of **1a** (0.01 mol%) is needed in this case to convert 0.5 mmol of nitrostyrene, whereas a similar conversion with common small molecule bifunctional catalyst would typically require >20 mg (10 mol%) of catalyst. As initially hypothesized, the catalytic process requires a relatively high concentration of base relative to the chiral catalyst, as

the reaction rate is significantly impacted at 1 mol% of Et<sub>3</sub>N (Table 1, entries 7 and 8). Conversely, increasing the concentration of Et<sub>3</sub>N to 20 and 30 mol% is well tolerated and allows shorter reaction times (Table 1, entries 9 and 10). The reaction with **1a**/Et<sub>3</sub>N was slightly less selective at RT (89% *ee*, entry 11). The synthetic utility of **1a** was further demonstrated by performing the reaction on a larger scale. Gram quantities of the Michael adduct (0.95 g after purification) and excellent *ee* (95% *ee*) were obtained when the reaction was conducted on a 3.3 mmol scale with 3.4 mg of **1a** (0.1 mol%).

Hexamer **2a**, which contains a thiourea at the first position, also performed well but was systematically less

effective than **1a** for the addition of malonate **3a** to the nitroolefin **4a** (Table 1, entry 12 vs entry 2 (at 24h) and entry 13 vs entry 11 (at RT)), suggesting a subtle interplay of acidity<sup>49</sup> and conformation in controlling the catalytic efficiency of the system. One plausible explanation is that the benefit of increasing the acidity by replacing the oxygen of the first urea by a sulfur atom may be counterbalanced by unfavorable conformational change and dynamics at the positive pole of the helix where catalysis takes place.<sup>42</sup>

**Catalysis upon folding: Chain-length dependence and temperature effects.** To investigate whether the helical conformation of oligo(thio)ureas **1a** and **2a** is critical to achieve rate acceleration and enantioselectivities reported in Table 1, we next prepared two series of shorter analogues (**1b-e** and **2c-e**) ranging from 1 to 5 monomeric (NHCH(R)-CH<sub>2</sub>-NHCO) units, and sharing the same terminal bis(thio)urea segment and 3,5-bis(trifluoromethyl)phenyl moiety (Fig. 3a). Whereas analogues consisting of one (**1e** and **2e**) and two (**1d** and **2d**) monomeric units are too short to adopt a helical conformation, longer analogues are expected to gradually populate the 2.5-helical conformation in non-polar and moderately polar

solvents.<sup>50</sup> The helix dipole is also expected to increase with the length of the helix, possibly suggesting a more pronounced interaction of longer oligomers with charged intermediates during the catalytic process. To gain more specific information about the helix forming propensity of oligoureas **1a-e**, we recorded their electronic circular dichroism (ECD) spectra in trifluoroethanol (Fig. 3b). As expected, the tetramer (**1c**), pentamer (**1b**) and hexamer (**1a**), but not dimer **1d** and monomer **1e**, displayed the characteristic ECD signature of (*P*)-2.5-helical oligoureas, with a positive maximum at ~203 nm whose intensity (mean residue ellipticity) increases with the number of residues in the chain. This observation was further supported by the degree of anisochronicity of NMR signals arising from diastereotopic protons in the chiral units of **1a-1e** (Supplementary Table 2). We obtained an X-ray crystal structure of 5-mer **1b**. This oligomer is fully helical in the crystal and an overlay with the structure of **1a** (Fig. 3c) by fitting the first five pairs of carbonyl C atoms indicates a very close match between the two helices including at the active site (root-mean-square deviation (RMSD) = 0.150 Å).

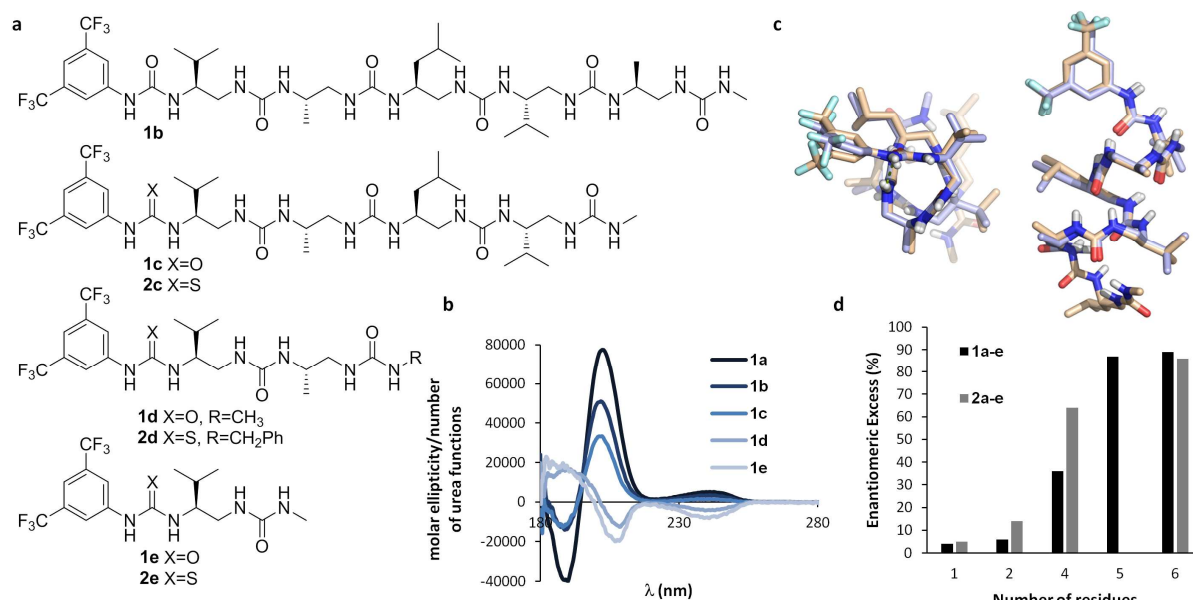


**Figure 3.** Catalysis and chain length dependence. a, Primary sequence of analogues of **1a** and **2a** ranging in size from monomer to pentamer. b, Electronic circular dichroism (ECD) analysis of oligoureas **1a-1e** in trifluoroethanol. Molar residual ellipticity in deg.cm<sup>2</sup>.dmol<sup>-1</sup>.residue<sup>-1</sup>. c, Structural alignment of the crystal structures of **1a** (carbon atoms in sand) and **1b** (carbon atoms in light blue). d, Enantiomeric excess of the Michael adduct **5** determined by chiral HPLC analysis after purification for reactions conducted in the presence of **1a-e** and **2a-e**. Reactions were performed at RT for 24h, with 0.1 mol% catalyst, 10 mol% Et<sub>3</sub>N, on 0.67 mmol scale.

All foldamers were then tested for their ability to catalyze the reaction between diethylmalonate **3a** with nitrostyrene **4a** at low chiral catalyst loading using

conditions reported in Table 1, entry 11 (chiral catalyst 0.1 mol%, Et<sub>3</sub>N 10 mol%, RT, 48 h). A strong chain length dependence effect was observed (Fig. 3d and

Supplementary Table 3) with almost no enantio-control in the presence of monomers (**1e** and **2e**) and dimers (**1d** and **2d**) and the highest reactivity (94-98% conversion) and selectivity (86-89 % *ee*) for helically folded 5- and 6-mers (**1a** > **1b** > **2a**). Intermediate selectivities (36-63 % *ee*) were obtained with partially folded 4-mers and in this case, conversion and stereocontrol were significantly higher with the thiourea containing derivative **2c**, suggesting that increased acidity of the catalyst could compensate for the limited conformational control. Overall these results support the view that a well-defined helical conformation is required for efficient stereocontrol in the catalytic process, and furthermore that even relatively short helices (e.g. 5-mer **1b**) display an excellent catalytic activity profile at low oligomer/substrate ratio. Because the 2.5-helix of oligoureas is robust and shows significant thermal stability in non-polar and moderately polar solvents,<sup>51</sup> we decided to evaluate to which extent the activity of the catalytic system **1a**/Et<sub>3</sub>N persists at high temperature. Although the selectivity gradually decreased between -20 and 80 °C the reactivity was not significantly affected, with the reaction at 80 °C still producing the Michael adduct in a satisfactory yield of 78% and 69% *ee*. This indicates that the active site as well as supramolecular interactions are largely maintained over a wide temperature range (Supplementary Fig. 2b).

**Scope of the reaction and fine tuning of the selectivity.** We next addressed the substrate scope of the reactions catalyzed by oligourea **1a** by applying it to other 1,3-dicarbonyl compounds and to a variety of nitroalkenes (Tables 2 and 3). The effectiveness of the catalyzed addition of malonate esters to nitrostyrene, in terms of reactivity and selectivity, inversely correlates with the size of the ester group; dimethyl malonate **3b** giving the fastest conversion and a remarkable 97% *ee*, and *tert*-butyl malonate **3e** being the least reactive (Supplementary Table 4, entries 1-5). When using cyclic ketoester **6** as a nucleophile, the resulting adduct **9** bearing a stereogenic quaternary center was formed with a high 98% *ee* and complete diastereoselectivity (Table 2, entry 1). As noted above, a distinctive feature of this synergistic approach as compared to the bifunctional catalyst approach is that variation of each catalyst component can be performed independently of the other. Thus, catalyst optimization may be simply achieved by modifying the nature of the associated Brønsted base. For example, during the initial scope of Michael donors, we observed that the reaction of acetylacetone **7** with nitrostyrene **4a** to produce adduct **10a**, (Table 2, entry 2) proceeded with a low 63% *ee* under our established conditions. However, the

reaction outcome could be significantly improved by employing trialkylamine bases with increasing alkyl chain length or bulkiness. Although we do not yet have a full explanation for this result, the data in Table 2 show that among the bases tested, *i*Pr<sub>2</sub>EtN (DIPEA) gave the best enantioselectivity for the addition reactions with acetylacetone **7** and 1,3-diphenylpropane-1,3-dione **8** with *ee*'s between 83 and >99 % (Table 2, entries 6, 9, 12 and 15).

**Table 2. Suitability of several 1,3-dicarbonyl compounds as nucleophiles and influence of the nature of the amine base cocatalyst.**

**6** (R<sup>1</sup>, R<sup>2</sup>=(CH<sub>2</sub>)<sub>4</sub>, R<sup>3</sup>=OMe)    **4a** (R=Ph)  
**7** (R<sup>1</sup>/R<sup>2</sup>=Me; R<sup>3</sup>=H)                **4b** (R=4-CH<sub>3</sub>C<sub>6</sub>H<sub>4</sub>)  
**8** (R<sup>1</sup>/R<sup>2</sup>=Ph; R<sup>3</sup>=H)                **4g** (R=4-ClC<sub>6</sub>H<sub>4</sub>)

Entry	Product	Amine base	Time (h)	Yield (%)	<i>ee</i> (%)
1		Et <sub>3</sub> N	40	72	98*
2		Et <sub>3</sub> N	16	92	63
3		<i>n</i> Bu <sub>3</sub> N	16	90	73
4		R':H ( <b>10a</b> ) <i>n</i> Hex <sub>3</sub> N	120	78	76
5		<i>n</i> Oct <sub>3</sub> N	120	72	83
6		<i>i</i> Pr <sub>2</sub> EtN	16	70	92
7		Et <sub>3</sub> N	16	82	80
8		R': Me ( <b>10b</b> ) <i>n</i> Oct <sub>3</sub> N	120	98	66
9		<i>i</i> Pr <sub>2</sub> EtN	16	90	86
10		Et <sub>3</sub> N	16	87	56
11		R': Cl ( <b>10g</b> ) <i>n</i> Oct <sub>3</sub> N	120	80	69
12		<i>i</i> Pr <sub>2</sub> EtN	16	82	83
13		Et <sub>3</sub> N	16	64	91
14		<i>n</i> Oct <sub>3</sub> N	72	99	95
15		<i>i</i> Pr <sub>2</sub> EtN	16	67	>99

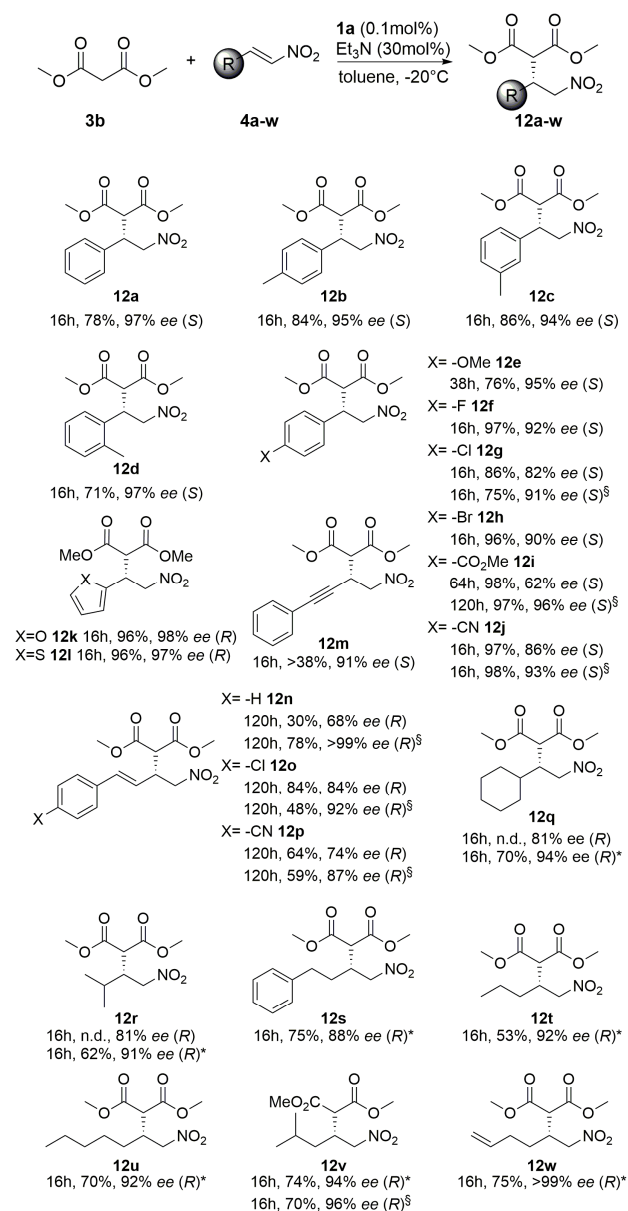
Reactions were performed on 1 mmol scale with 2 equiv. of diketone. Yields correspond to isolated compound after chromatographic purification. The *ee* was determined by chiral HPLC analysis. Absolute configuration (*R*) or (*S*) was known or assigned by analogy. \**dr* (2*R*/2*S*) : 0:100

As shown in Table 3, the catalyzed reaction of dimethyl malonate **3b** with an array of nitroalkenes **4** was found to be quite independent of the electronic

properties of the aryl ring of the nitroalkene. Compound **4a** as well as nitroalkenes with electron donating  $\beta$ -aryl groups such as **4b**, **4c**, **4d** and **4e** led to the corresponding adducts **12a-e** with excellent chemical and stereochemical results, regardless of their *o*-, *m*- or *p*-substitution pattern. Likewise, nitroalkenes **4f**, **4g** and **4h** with inductively electron withdrawing fluoro, chloro and bromo groups afforded Michael adducts **12f-h** with good yields and *ee*'s up to 92%. Somewhat inferior results were observed for the reaction of **4i** and **4j**, bearing electron poor  $\beta$ -aryl groups, which provided adducts **12i** and **12j** with 62% *ee* and 86% *ee*, respectively. In these cases, the enantioselectivity was largely improved by using DIPEA as a base (96% and 93% *ee*, respectively) instead of Et<sub>3</sub>N. Nitroalkenes with heteroaromatic  $\beta$ -substituents such as **4k** and **4l** are also good acceptors, and provide the corresponding adducts **12k** and **12l** in 98% *ee* and 97% *ee*, respectively. Conjugated nitroalkenes **4m-p** led to the respective adducts **12m-p**, although long reaction times were required. Again, the combination of DIPEA with **1a** proved superior to the use of Et<sub>3</sub>N in terms of stereocontrol (e.g. **12n-12p**). Importantly, only 0.1 mol % of catalyst loading was needed in the majority of the cases in order to achieve good yields of isolated product and high enantioselectivities. To the best of our knowledge, this represents the lowest catalyst/substrate ratio employed in Brønsted base catalyzed Michael reaction of malonate esters to nitroalkenes.<sup>33-52,53</sup> Most significantly, the recalcitrant  $\beta$ -alkyl nitroalkenes such as **4q** and **4r**, which generally lead to sluggish reactions and poor *ee*'s,<sup>34,35</sup> provided the corresponding adducts with *ee*'s up to 81% at 0.1 mol% catalyst loading and -20 °C. In these cases, the enantioselectivity could be substantially improved by increasing the amount of catalyst to 0.3 mol% and decreasing the reaction temperature to -30 °C. As shown in Table 3, extension to nitroalkenes **4s-w** with short, large and ramified  $\beta$ -alkyl chains is equally tolerated and provided adducts **12s-w** in good yields and high *ee*'s.

**Structure-reactivity/enantioselectivity relationship and mechanistic studies.** We conducted analysis by <sup>1</sup>H NMR in toluene-d<sub>8</sub> of mixtures of **1a**, Et<sub>3</sub>N, **3a** and **4a** in order to generate information concerning the kinetics of the foldamer-catalyzed addition reaction of malonate to nitroolefin (Supplementary Figure 3). Using the method of flooding with [3a] = 10 × [4a], we confirm that the reaction exhibits a first-order with respect to nitrostyrene. The method of initial rates was used to determine the order in foldamer, base and malonate **3a**.<sup>54</sup> We found that the reaction is first order with respect to base and malonate **3a** and also exhibit a first order dependence in foldamer at concentrations below ≈ 0.2 mol%.

**Table 3. Scope of the enantioselective conjugate addition of dimethylmalonate to nitroalkenes catalyzed by **1a****



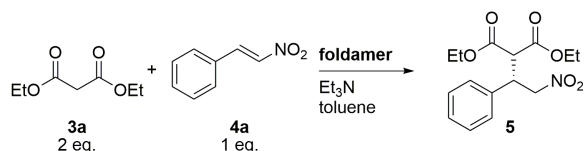
Reactions were performed on 0.5 mmol scale with 2 equiv. of **3b**. Yields correspond to isolated compound after chromatographic purification and are given in per cent. The *ee* was determined by chiral HPLC analysis. Absolute configuration (R) or (S) was known or assigned by analogy. <sup>§</sup>The reaction was performed using DIPEA as base (30 mol%); \*Reaction conducted at -30 °C using 0.3 mol% catalyst.

The deviations from first order kinetics at higher concentrations of **1a** could be rationalized by a possible aggregation of the foldamer, an explanation which is also supported by the small but substantial non-linear effect which is observed at 0.1 mol% when the *ee* of the catalyst is varied by mixing **1** and its enantiomer *ent-1* in defined proportions (Supplementary Fig. 4).

We next introduced sequence variations into **1a** and **2a** in order to interrogate the role of the first two (thio)urea moieties and gain additional insight into the principles governing the catalytic activity of oligoureas as a mean to improve next generation foldamer-based catalysts (Fig. 4). Pyrrolidine units in compounds **13-15** were used to selectively block the first or second accessible urea groups. The crystal structures of **15** (Fig. 4b) and of the Boc-protected precursor of **14** (compound **2o**, Supplementary Fig. 1c) show that the

geometry of the 2.5-helix is compatible with the introduction of a pyrrolidine unit. In the crystal, the CO-N-C $\beta$ -C $\alpha$  angle ( $\phi$ ) of the pyrrolidine units adopts a value ( $\approx -96^\circ$ ) close to that of standard residues in helical oligoureas and the carbonyl group of the pyrrolidine unit is engaged in typical H-bonds with urea NHs of canonical residues. Helix formation is also supported in solution by anisochronicities measured in the chiral units of compounds **13-15**, although with some local perturbation at the site of the pyrrolidine insertion (Fig. 4c). Despite the overall structural similarity between **14** / **15** and **1a** / **2a** respectively, we found that the pyrrolidine residues in **14** and **15** were detrimental to the catalytic activity ( $\approx 35\%$  and  $15\%$  conversion, respectively) supporting a key role of the second urea site in catalysis (Table 4, entries 2 and 3).

**Table 4. Correlation of the foldamer structure with the catalytic activity.**



Entry	Chiral Catalyst	Foldamer Loading (mol%)	Temperature (°C)	Reaction Time (h)	Et <sub>3</sub> N (mol%)	Conversion (%)	Yield (%)	ee (%)
1	<b>13</b>	0.1	-20	48	10	72	47	57
2	<b>14</b>	0.1	-20	48	10	35	29	5
3	<b>15</b>	0.1	-20	48	10	15	n.d.	15
4	<b>16</b>	0.1	-20	48	10	62	48	68
5	<b>17</b>	0.1	-20	48	10	92	75	83
6	<b>18</b>	0.1	-20	48	10	45	40	35
7	<b>19</b>	0.1	-20	48	10	94	75	88

Reactions were performed with 0.5 mmol of **4a** and 1.0 mmol of **3a**. Yields correspond to isolated compound after chromatographic purification. The enantiomeric excess (*ee*) was determined by chiral HPLC analysis. Absolute configuration (*R*) or (*S*) was known or assigned by analogy.

The combination of oligourea **13** and Et<sub>3</sub>N was more active, providing the Michael adduct in a moderate yield and 57% *ee* (Table 4, entry 1) which suggests that the replacement of the first chiral residue with a pyrrolidine unit is less critical to catalytic activity. The role of the first urea group in the catalytic process was further investigated by decreasing its acidic strength through replacement of the 3,5-bis(trifluoromethyl)phenyl termination with a 4-Br-phenyl group. This modification (**16**) leads to a similar outcome as to the pyrrolidine ring insertion at the first urea position (**13**), with a moderate yield and 68 % *ee*

(Table 4, entry 4). These data support a cooperative role of both ureas in the catalytic process.

We next probed the contribution of the stereocenter of the first chiral residue on the catalytic process by either removing the branched side-chain (**17** and **18**) or replacing it with a benzyl group (**19**). The combination of two potentially destabilizing elements at the end of the helix, i.e. a flexible achiral 1,2-diaminoethyl residue<sup>55</sup> and a thiourea termination<sup>42</sup> (Fig. 4a) in **18** was deleterious for the catalytic efficiency and resulted in poor conversion and stereocontrol (Table 4, entry 6). Interestingly, oligourea **17** which has a urea termination, still produces the Michael adduct in good yield and

selectivity (83% *ee*), providing evidence that the stereochemical outcome of the reaction largely depends on the helical nature of the catalyst and is not significantly controlled locally by the first chiral unit

(Table 4, entry 5). In line with this result, catalyst **19** was found to behave similarly to **1a** but with a slightly lower degree of stereocontrol (Table 4, entry 7).

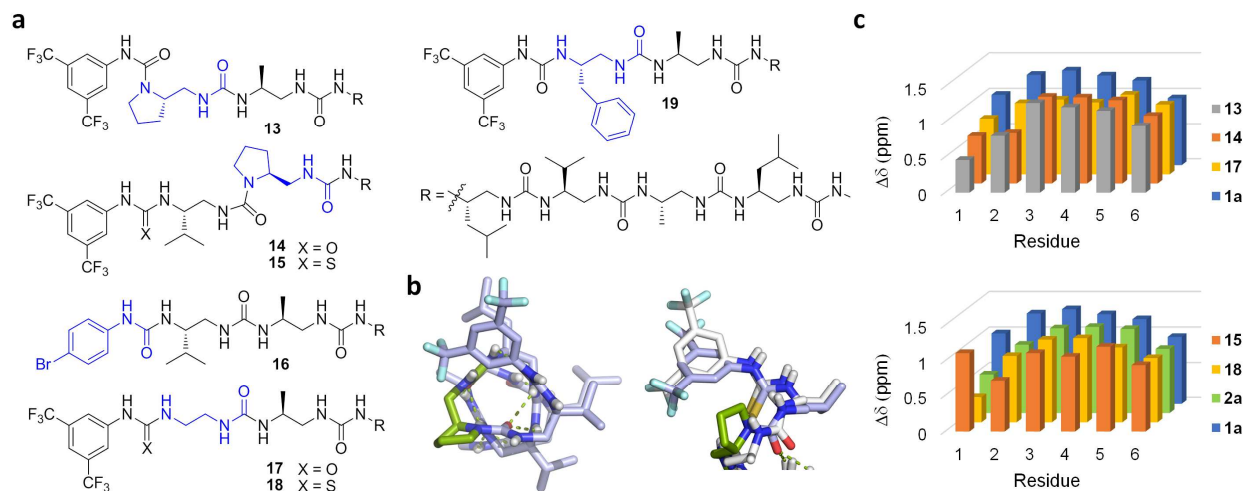


**Figure 4.** Oligomer sequences for structure-reactivity/enantioselectivity relationship study. a, Analogues of **1a** and **2a** bearing various sequence variations at the first two positions: pyrrolidine residue replacements (**13-15**), terminal aromatic group modification (**16**), achiral 1,2-diaminoethyl residue replacement (**17, 18**) and benzyl side chain replacement (**19**). b, Crystal structure of compound **15** with a pyrrolidine residue at the second position viewed down helix axis and superimposition with the structure of **2a** (RMSD = 0.460 Å by fitting the seven pairs of (thio)carbonyl C atoms). The pyrrolidine residue is colored in green. c, Anisochronicity in the residues of catalysts **13-15** and **17-18** compared to that of catalysts **1a** and **2a**. The values have been measured in CD<sub>3</sub>OH for all compounds except **17** for which NMR analysis was conducted in DMSO-d<sub>6</sub>.

## Conclusions

We report here the first successful development of customizable foldamers – aliphatic N,N'-linked oligoureas – as critical chiral components of synergistic catalytic systems (achiral base/chiral H-bond donor foldamer catalyst) for enabling efficient simultaneous activation of the nucleophile and the electrophile at extremely low catalyst/substrate molar ratios. As little as 0.01 mol% of foldamer **1a** in combination with 10 mol % Et<sub>3</sub>N was shown to be sufficient to catalyze the addition of 1,3-dicarbonyl substrates to nitroalkenes in high yield and enantioselectivity. This system is highly robust and, crucially, enables facile optimization, due to the separation of base and H-bond donor components of the catalyst system. For example, the use of DIPEA (instead of Et<sub>3</sub>N) in combination with **1a** was subsequently found to substantially increase enantioselectivity in the most difficult cases. Other modular binary systems albeit non chiral, such as a simple (thio)urea and a base component have proven particularly versatile in macromolecular catalysis for ring opening polymerization of lactide.<sup>52,56</sup> Furthermore, we gained insight into the mechanisms and origins of the high selectivity observed by varying the chiral catalyst primary sequence, folding propensity, and by

introducing urea → thiourea replacements. This structure/activity relationship study revealed a strong correlation between the oligomer catalyst efficiency and its folding propensity in apolar and moderately polar solvents. It also supports a key role for the first two (thio)ureas close to the positive pole of the helix macrodipole, which is reminiscent of the role of amide NHs at the positive pole (N-terminus) of the helical poly-leucine catalyst used in the Juliá-Colonna epoxidation.<sup>11,57</sup>

The chiral oligourea foldamers studied here combine a number of unique and positive features – such as synthetic accessibility, functional capability, sequence modularity, and high folding fidelity – which could be further applied to catalysis of other C-C bond forming reactions, or even turned into distinct practical and scalable technologies. Overall the present development provides new insights into the factors that govern catalysis of organic reactions by middle size molecules and thus constitutes a new step towards approaching the efficiency of enzymes.

## Methods

**General procedure for the synthesis of oligo(thio)ureas.** Oligomers **1, 2** and **13-19** and *ent-1*

1  
2  
3 were synthesized in solution using a stepwise approach  
4 and N-Boc protected succinimidyl carbamate building  
5 blocks following previously reported procedures.<sup>27,55</sup>  
6 Full details of chemical synthesis and purification can  
7 be found in the Supplementary Information.

8  
9 **Hexamer 1a.** Trifluoroacetic acid (2 mL) was added  
10 to a solution of the corresponding Boc-protected  
11 oligourea hexamer (800 mg, 0.88 mmol) in  
12 dichloromethane (2 mL) and the reaction mixture was  
13 stirred at room temperature for 4 h. After completion of  
14 the reaction, trifluoroacetic acid and dichloromethane  
15 were evaporated under reduced pressure. DIPEA (0.48  
16 mL, 2.72 mmol) and 3,5-bis(trifluoromethyl)phenyl  
17 isocyanate (0.24 mL, 1.36 mmol) were successively  
18 added to the resulting TFA salt dissolved in DMF (4  
19 mL). The reaction mixture was stirred at room  
20 temperature for 16 h. Sodium bicarbonate solution (30  
21 mL) was added which led to gel formation which was  
22 recovered after filtration, then dissolved in methanol,  
23 concentrated and dried under high vacuum. The  
24 recovered orange solid was triturated in acetonitrile to  
25 lead to the titled oligourea **1a** as a white solid (731 mg,  
26 81%). <sup>1</sup>H NMR (400 MHz, CD<sub>3</sub>OH) δ (ppm) 9.01 (s, 1H),  
27 8.00 (brs, 2H), 7.52 (brs, 1H), 6.56 (dd, J = 10.2 and 2.7  
28 Hz, 1H), 6.50 (dd, J = 9.8 and 2.3 Hz, 1H), 6.37-6.45 (m,  
29 2H), 6.26 (d, J = 10.7 Hz, 1H), 6.24 (d, J = 10.3 Hz, 1H),  
30 6.21 (q, J = 4.9 Hz, 1H), 6.03-6.11 (m, 2H), 6.00 (dd, J =  
31 9.6 and 3.6 Hz, 1H), 5.97 (d, J = 10.6 Hz, 1H), 5.93 (d, J =  
32 10.6 Hz, 1H), 5.86 (d, J = 10.1 Hz, 1H), 4.00-4.15 (m, 1H),  
33 3.75-4.00 (m, 4H), 3.48-3.75 (m, 7H), 2.70 (d, J = 4.8 Hz,  
34 3H), 2.57-2.74 (m, 2H), 2.24-2.47 (m, 4H), 1.64-1.85 (m,  
35 3H), 1.49-1.64 (m, 1H), 1.12-1.32 (m, 4H), 1.00-1.06 (m,  
36 9H), 0.98 (d, J = 7.0 Hz, 3H), 0.88-0.95 (m, 15 H), 0.86  
37 (d, J = 7.0 Hz, 3H); <sup>13</sup>C NMR (100 MHz, CD<sub>3</sub>OH) δ (ppm)  
38 162.1 (C), 162.0 (C), 161.8 (C), 161.6 (C), 161.4 (C), 160.9  
39 (C), 158.2 (C), 143.2 (C), 133.1 (q, J = 33 Hz, 2 × C), 124.6  
40 (q, J = 270 Hz, 2 × C), 118.8-119.1 (m, 2 × CH), 115.5-115.8  
41 (m, CH), 56.7 (CH), 56.2 (CH), 49.4 (CH), 49.1 (CH),  
42 48.2 (2 × CH<sub>2</sub>), 47.3 (CH<sub>2</sub>), 46.8 (CH), 46.3 (CH<sub>2</sub>), 46.1  
43 (CH), 44.7 (CH<sub>2</sub>), 44.4 (CH<sub>2</sub>), 43.8 (CH<sub>2</sub>), 42.7 (CH<sub>2</sub>),  
44 31.91 (CH), 31.88 (CH), 26.8 (CH<sub>3</sub>), 26.1 (CH), 25.8 (CH),  
45 23.6 (CH<sub>3</sub>), 23.5 (CH<sub>3</sub>), 22.7 (CH<sub>3</sub>), 22.4 (CH<sub>3</sub>), 20.1  
46 (CH<sub>3</sub>), 20.0 (CH<sub>3</sub>), 18.7 (CH<sub>3</sub>), 18.5 (CH<sub>3</sub>), 18.3 (CH<sub>3</sub>),  
47 18.2 (CH<sub>3</sub>); <sup>19</sup>F NMR (376 MHz, CD<sub>3</sub>OH) δ (ppm) -64.6  
48 ppm; HRMS (ES<sup>+</sup>, MeOH) calcd for C<sub>44</sub>H<sub>76</sub>F<sub>6</sub>N<sub>14</sub>O<sub>7</sub> =  
49 1027.59984; found 1027.60173.

50 **General procedure for the catalytic**  
51 **enantioselective conjugate addition of dimethyl**  
52 **malonate to nitroalkenes (Table 3).** To a vial charged  
53 with **1a** (0.51 mg, 0.5 μmol) were added the nitroalkene  
54 (0.5 mmol) and a solution of freshly distilled dimethyl  
55 malonate (0.11 mL, 1.0 mmol) in dry toluene (0.5 mL).  
56 The reaction mixture was cooled down to -20 °C and  
57 tertiary amine (0.15 mmol) was added. After complete

consumption of the nitroalkene, the reaction mixture  
was quenched with 1N hydrochloric acid solution,  
extracted three times with dichloromethane, washed  
with brine, dried over magnesium sulfate, filtered and  
concentrated. The crude material was purified on silica  
gel chromatography as described in Supporting  
Information. The enantiomeric excess was determined  
by chiral HPLC as described in Supplementary  
Information.

**Circular Dichroism.** ECD experiments were  
performed on a Jasco J-815 spectrometer. Measurements  
on oligoureas **1a-e** and **2a-e** were performed at 2 mM in  
trifluoroethanol. Solutions with different ratios **1a** / ent-  
**1a** were obtained from a mixture of stock solutions of **1a**  
and ent-**1a** to lead to a final concentration of 2 mM in  
oligourea. Data were recorded at 20 °C between  
wavelengths of 180 and 250 nm at 0.5 nm intervals at a  
speed of 50 nm min<sup>-1</sup> with an integration time of two  
seconds.

**X-ray diffraction.** Atomic coordinates and structure  
factors have been deposited in the Cambridge  
Crystallographic Data Centre with accession codes:  
1534525, 1534527, 1534523, 1534528, and 1534526, for  
structures **1a**, **1b**, **2a**, **15**, and **20** respectively, and can be  
obtained free of charge upon request  
([www.ccdc.cam.ac.uk/data\\_request/](http://www.ccdc.cam.ac.uk/data_request/)).

## ASSOCIATED CONTENT

\*Supporting Information

Additional experimental procedures and characterization  
data of all compounds, supplemental Figures S1–S19 and  
Tables S1–S23 (PDF)

Crystallographic data for **1a** (CIF)

Crystallographic data for **1b** (CIF)

Crystallographic data for **2a** (CIF)

Crystallographic data for **15** (CIF)

Crystallographic data for **20** (CIF)

## AUTHOR INFORMATION

### Corresponding Author

\* g.guichard@iecb.u-bordeaux.fr

\* claudio.palomo@ehu.es

### ORCID

Gilles Guichard: 0000-0002-2584-7502

Claudio Palomo: 0000-0001-9809-2799

**Present Address:**

¶ Current address: UMR CNRS 8161 Pasteur Institute of Lille, Univ Lille, 1 rue du Pr Calmette, 59021 Lille, France

**Notes**

The authors declare no competing financial interest.

**ACKNOWLEDGEMENTS**

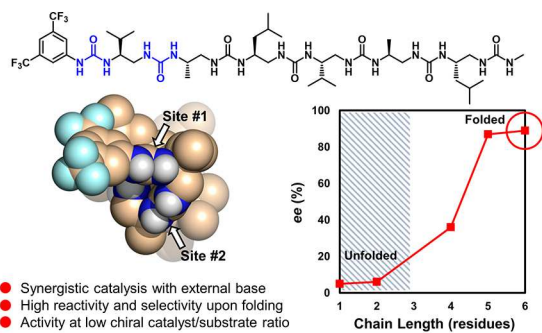
This work is dedicated to Prof. Dieter Seebach on the occasion of his 80<sup>th</sup> Birthday. The work was funded in part by the CNRS, ANR (ANR-10-PDOC-0022), Conseil Regional d'Aquitaine (Project #2014-1R10208), UREkA and in part by MEC (CTQ2014-62203-EXP, Spain). A pre-doctoral fellowship from the IDEX of Univ. Bordeaux to D. B. is gratefully acknowledged (funding from the French National Research Agency - Program ANR No.-10-IDEX-03-02). This work has benefited from the facilities and expertise of IECB Biophysical and Structural Chemistry platform (BPCS), CNRS UMS3033, Inserm US001, Univ. Bordeaux.

**REFERENCES**

- (1) Guichard, G.; Huc, I. *Chem. Commun.* **2011**, *47*, 5933-5941.
- (2) Checco, J. W.; Gellman, S. H. *Curr. Opin. Struc. Biol.* **2016**, *39*, 96-105.
- (3) Chandramouli, N.; Ferrand, Y.; Lautrette, G.; Kauffmann, B.; Mackereth, C. D.; Laguerre, M.; Dubreuil, D.; Huc, I. *Nat Chem* **2015**, *7*, 334-341.
- (4) Juwarker, H.; Suk, J. M.; Jeong, K. S. *Chem. Soc. Rev.* **2009**, *38*, 3316-3325.
- (5) Wang, P. S. P.; Schepartz, A. *Chem. Commun.* **2016**, *52*, 7420-7432.
- (6) Horne, W. S. *Nat. Chem.* **2015**, *7*, 858-859.
- (7) Ringe, D.; Petsko, G. A. *Science* **2008**, *320*, 1428-1429.
- (8) Jones, C. R.; Pantos, G. D.; Morrison, A. J.; Smith, M. D. *Angew. Chem. Int. Ed. Engl.* **2009**, *48*, 7391-7394.
- (9) Davie, E. A. C.; Mennen, S. M.; Xu, Y.; Miller, S. J. *Chem. Rev.* **2007**, *107*, 5759-5812.
- (10) Lewandowski, B.; Wennemers, H. *Curr. Opin. Chem. Biol.* **2014**, *22*, 40-46.
- (11) Berkessel, A.; Gasch, N.; Glaubitz, K.; Koch, C. *Org. Lett.* **2001**, *3*, 3839-3842.
- (12) Akagawa, K.; Kudo, K. *Angew. Chem. Int. Ed.* **2012**, *51*, 12786-12789.
- (13) Burton, A. J.; Thomson, A. R.; Dawson, W. M.; Brady, R. L.; Woolfson, D. N. *Nat. Chem.* **2016**, *8*, 837-844.
- (14) Coffey, P. E.; Drauz, K.-H.; Roberts, S. M.; Skidmore, J.; Smith, J. A. *Chem. Commun.* **2001**, 2330-2331.
- (15) Hasegawa, T.; Furusho, Y.; Katagiri, H.; Yashima, E. *Angew. Chem. Int. Ed.* **2007**, *46*, 5885-5888.
- (16) Maayan, G.; Ward, M. D.; Kirshenbaum, K. *Proc. Nat. Acad. Sci. U.S.A.* **2009**, *106*, 13679-13684.
- (17) Müller, M. M.; Windsor, M. A.; Pomerantz, W. C.; Gellman, S. H.; Hilvert, D. *Angew. Chem. Int. Ed.* **2009**, *48*, 922-925.
- (18) Wang, P. S. P.; Nguyen, J. B.; Schepartz, A. *J. Am. Chem. Soc.* **2014**, *136*, 6810-6813.
- (19) Le Bailly, B. A. F.; Byrne, L.; Clayden, J. *Angew. Chem. Int. Ed.* **2016**, *55*, 2132-2136.
- (20) Burgess, K.; Ibarzo, J.; Linthicum, D. S.; Russell, D. H.; Shin, H.; Shitangkoon, A.; Totani, R.; Zhang, A. J. *J. Am. Chem. Soc.* **1997**, *119*, 1556-1564.
- (21) Semetey, V.; Rognan, D.; Hemmerlin, C.; Graff, R.; Briand, J.-P.; Marraud, M.; Guichard, G. *Angew. Chem. Int. Ed.* **2002**, *41*, 1893-1895.
- (22) Fischer, L.; Guichard, G. *Org. Biomol. Chem.* **2010**, *8*, 3101-3117.
- (23) Fremaux, J.; Mauran, L.; Pulka-Ziach, K.; Kauffmann, B.; Odaert, B.; Guichard, G. *Angew. Chem. Int. Ed.* **2015**, *54*, 9816-9820.
- (24) Collie, G. W.; Pulka-Ziach, K.; Lombardo, C. M.; Fremaux, J.; Rosu, F.; Decossas, M.; Mauran, L.; Lambert, O.; Gabelica, V.; Mackereth, C. D.; Guichard, G. *Nat. Chem.* **2015**, *7*, 871-878.
- (25) Teyssières, E.; Corre, J.-P.; Antunes, S.; Rougeot, C.; Dugave, C.; Jouvion, G.; Claudon, P.; Mikaty, G.; Douat, C.; Goossens, P. L.; Guichard, G. *J. Med. Chem.* **2016**, *59*, 8221-8232.
- (26) Collie, G. W.; Bailly, R.; Pulka-Ziach, K.; Lombardo, C. M.; Mauran, L.; Taib-Maamar, N.; Dessolin, J.; Mackereth, C. D.; Guichard, G. *J. Am. Chem. Soc.* **2017**, *139*, 6128-6137.
- (27) Diemer, V.; Fischer, L.; Kauffmann, B.; Guichard, G. *Chem. Eur. J.* **2016**, *22*, 15684-15692.
- (28) Wechsel, R.; Raftery, J.; Cavagnat, D.; Guichard, G.; Clayden, J. *Angew. Chem. Int. Ed.* **2016**, *55*, 9657-9661.
- (29) Zhang, Z.; Schreiner, P. R. *Chem. Soc. Rev.* **2009**, *38*, 1187-1198.
- (30) Stone, M. T.; Heemstra, J. M.; Moore, J. S. *Acc. Chem. Res.* **2006**, *39*, 11-20.
- (31) Doyle, A. G.; Jacobsen, E. N. *Chem. Rev.* **2007**, *107*, 5713-5743.
- (32) Wenzel, A. G.; Jacobsen, E. N. *J. Am. Chem. Soc.* **2002**, *124*, 12964-12965.
- (33) Okino, T.; Hoashi, Y.; Takemoto, Y. *J. Am. Chem. Soc.* **2003**, *125*, 12672-12673.
- (34) Okino, T.; Hoashi, Y.; Furukawa, T.; Xu, X.; Takemoto, Y. *J. Am. Chem. Soc.* **2005**, *127*, 119-125.
- (35) (a) McCooey, S. H.; Connon, S. J. *Angew. Chem. Int. Ed.* **2005**, *44*, 6367-6370; (b) Ye, J.; Dixon, D. J.; Hynes, P. S. *Chem. Commun.* **2005**, 4481-4483; (c) Vakulya, B.; Varga, S.; Csámpai, A.; Soós, T. *Org. Lett.* **2005**, *7*, 1967-1969.
- (36) Palomo, C.; Oiarbide, M.; Lopez, R. *Chem. Soc. Rev.* **2009**, *38*, 632-653.
- (37) Probst, N.; Madarász, Á.; Valkonen, A.; Pápai, I.; Rissanen, K.; Neuvonen, A.; Pihko, P. M. *Angew. Chem. Int. Ed.* **2012**, *51*, 8495-8499.
- (38) *Science of Synthesis: Asymmetric Organocatalysis Vol. 2: Bronsted Base and Acid Catalysts, and Additional Topics*; Maruoka, K., Ed.; Thieme Publishing Group Stuttgart, Germany, 2012.
- (39) Kennedy, C. R.; Lehnher, D.; Rajapaksa, N. S.; Ford, D. D.; Park, Y.; Jacobsen, E. N. *J. Am. Chem. Soc.* **2016**, *138*, 13525-13528.
- (40) Neuvonen, A. J.; Földes, T.; Madarász, Á.; Pápai, I.; Pihko, P. M. *ACS Catal.* **2017**, *7*, 3284-3294.
- (41) Allen, A. E.; MacMillan, D. W. C. *Chem. Sci.* **2012**, *3*, 633-658.
- (42) Nelli, Y. R.; Antunes, S.; Salaün, A.; Thinon, E.; Massip, S.; Kauffmann, B.; Douat, C.; Guichard, G. *Chem. Eur. J.* **2015**, *21*, 2870-2880.
- (43) *Organocatalytic Enantioselective Conjugate Addition Reactions: A Powerful Tool for the Stereocontrolled Synthesis of Complex Molecules*; Vicario, J. L.; Badia, D.; Carrillo, L.; Reyes, E., Eds.; The Royal Society of Chemistry: Cambridge, 2010; Vol. 5.

- 1  
2  
3 (44) Berner, Otto M.; Tedeschi, L.; Enders, D. *European*  
4 *Journal of Organic Chemistry* **2002**, 2002, 1877-1894.  
5 (45) Aitken, L. S.; Arezki, N. R.; Dell'Isola, A.; Cobb, A. J.  
6 *A. Synthesis* **2013**, 45, 2627-2648.  
7 (46) Sukhorukov, A. Y.; Sukhanova, A. A.; Zlotin, S. G.  
8 *Tetrahedron* **2016**, 72, 6191-6281.  
9 (47) Right-handed (*P*) foldamers **1a** and **2a** provided the (*S*)-  
10 adduct.  
11 (48) It is noteworthy that the present synergistic catalysis  
12 system appears to be more efficient than standard bifunctional  
13 Brønsted base/H-bond catalysts for this particular transformation.  
14 See the Supplementary Information for details.  
15 (49) Jakab, G.; Tancon, C.; Zhang, Z.; Lippert, K. M.;  
16 Schreiner, P. R. *Org. Lett.* **2012**, 14, 1724-1727.  
17 (50) Violette, A.; Lancelot, N.; Poschalko, A.; Piotto, M.;  
18 Briand, J. P.; Raya, J.; Elbayed, K.; Bianco, A.; Guichard, G.  
19 *Chem. Eur. J.* **2008**, 14, 3874-3882.  
20 (51) Hemmerlin, C.; Marraud, M.; Rognan, D.; Graff, R.;  
21 Semetey, V.; Briand, J.-P.; Guichard, G. *Helv. Chim. Acta* **2002**,  
22 85, 3692-3711.  
23 (52) Lin, B.; Waymouth, R. M. *J. Am. Chem. Soc.* **2017**, 139,  
24 1645-1652.  
25 (53) Giacalone, F.; Gruttadauria, M.; Agrigento, P.; Noto, R.  
26 *Chem. Soc. Rev.* **2012**, 41, 2406-2447.  
27 (54) Quintard, A.; Cheshmedzhieva, D.; Sanchez Duque, M.  
28 d. M.; Gaudel-Siri, A.; Naubron, J.-V.; Génisson, Y.; Plaquevent,  
29 J.-C.; Bugaut, X.; Rodriguez, J.; Constantieux, T. *Chem. Eur. J.*  
30 **2015**, 21, 778-790.  
31 (55) Pendem, N.; Douat, C.; Claudon, P.; Laguerre, M.;  
32 Castano, S.; Desbat, B.; Cavagnat, D.; Ennifar, E.; Kauffmann, B.;  
33 Guichard, G. *J. Am. Chem. Soc.* **2013**, 135, 4884-4892.  
34 (56) Zhang, X.; Jones, G. O.; Hedrick, J. L.; Waymouth, R.  
35 M. *Nat Chem* **2016**, 8, 1047-1053.  
36 (57) Kelly, D. R.; Roberts, S. M. *Chem. Commun.* **2004**,  
37 2018-2020.  
38  
39  
40  
41  
42  
43  
44  
45  
46  
47  
48  
49  
50  
51  
52  
53  
54  
55  
56  
57  
58  
59  
60

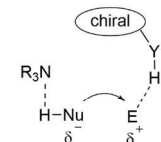
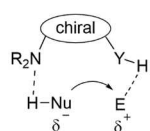
## TOC



## a Strategies for dual activation of nucleophile and electrophile

Bifunctional activation

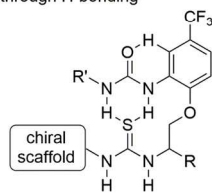
Synergistic activation



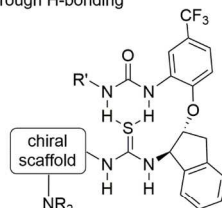
## b Improving the catalytic profile of thiourea catalysts

Chiral H-bond small molecule catalyst preorganized through H-bonding

Bifunctional H-bond small molecule catalyst preorganized through H-bonding



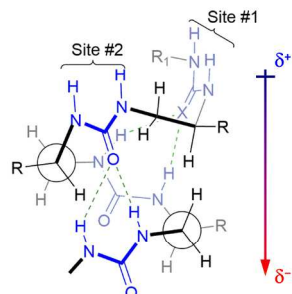
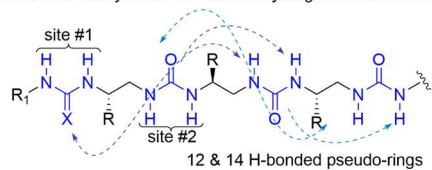
(Smith, 2009)



(Pihko, 2012)

## c This work

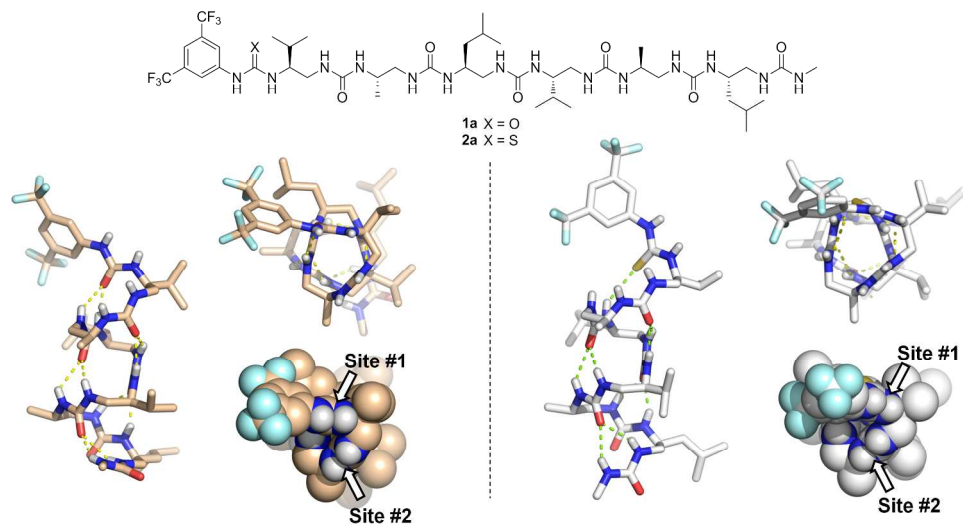
Helical foldamer catalyst with two distinct hydrogen bond donor sites



- Preorganization based on folding
- Two distinct recognition sites (different pKa depending on R<sup>1</sup>)
- Controlled distance and orientation between sites #1 & #2
- Contribution of the helix macrodipole

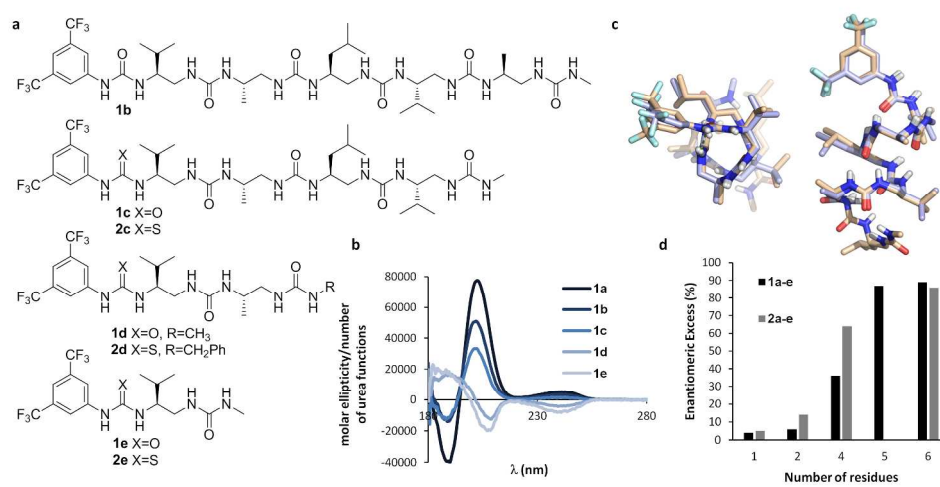
High resolution Figure 1

124x254mm (300 x 300 DPI)



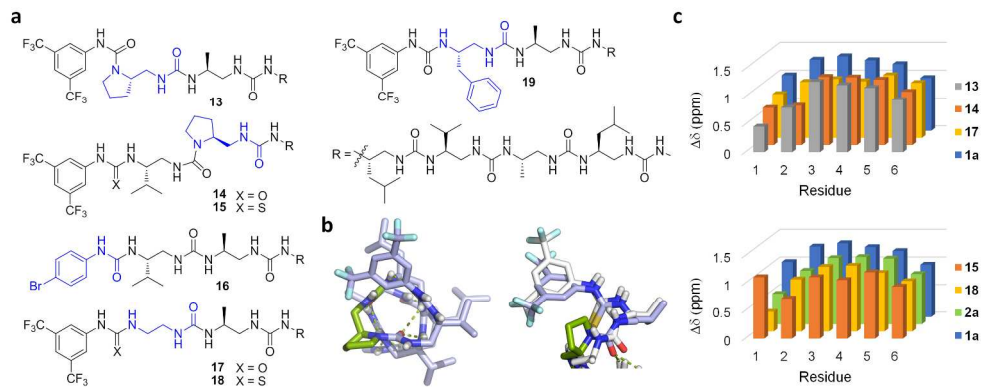
High resolution Figure 2

250x134mm (300 x 300 DPI)



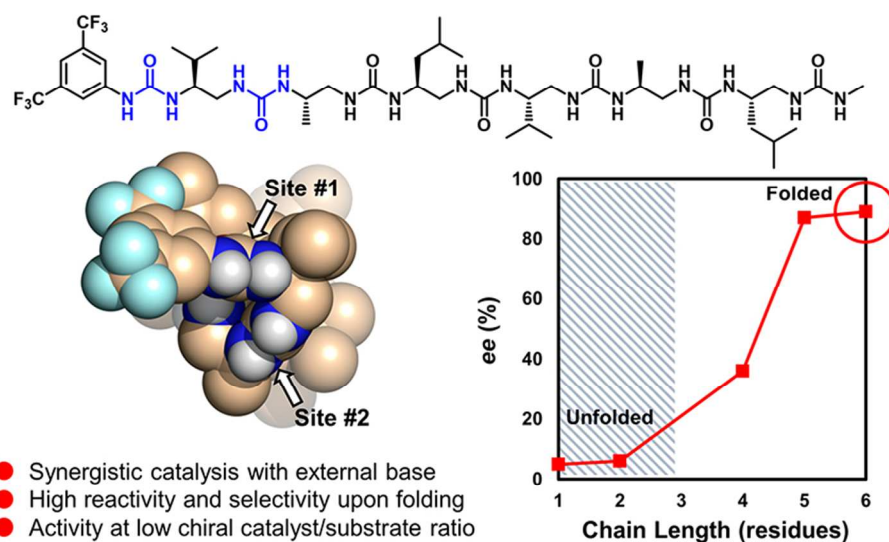
High resolution Figure 3

254x124mm (300 x 300 DPI)



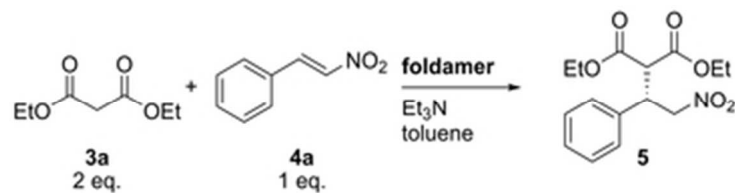
High resolution Figure 4

245x99mm (300 x 300 DPI)



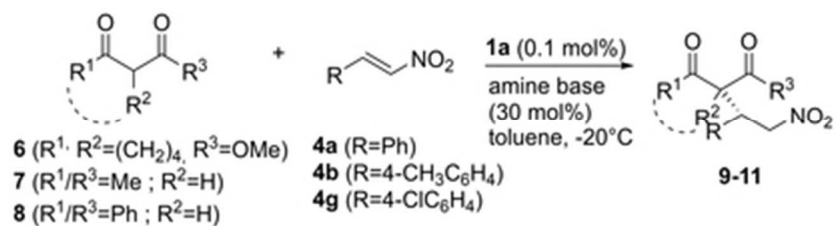
High resolution Table of Content graphic

79x47mm (300 x 300 DPI)



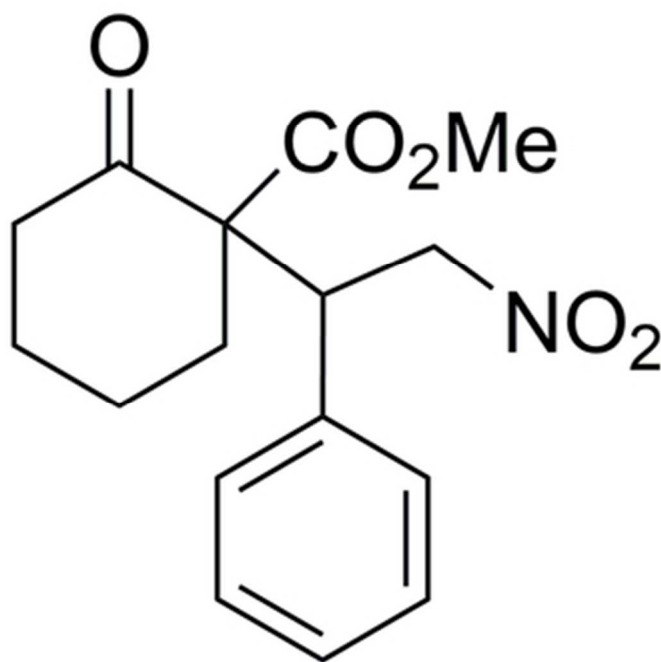
High res (600 dpi) scheme for Table 1

30x8mm (300 x 300 DPI)



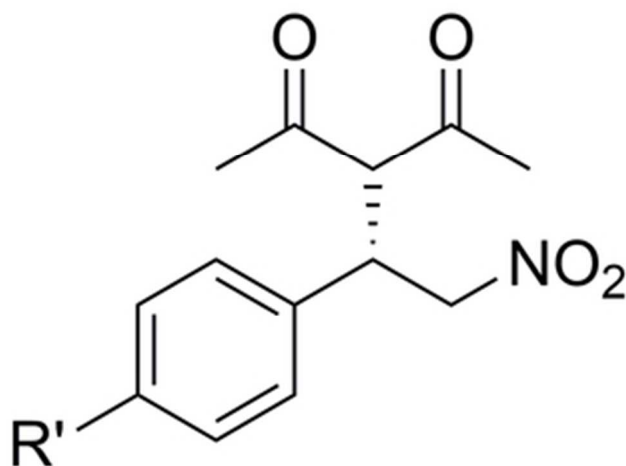
High res (600 dpi) scheme for Table 2

35x9mm (300 x 300 DPI)



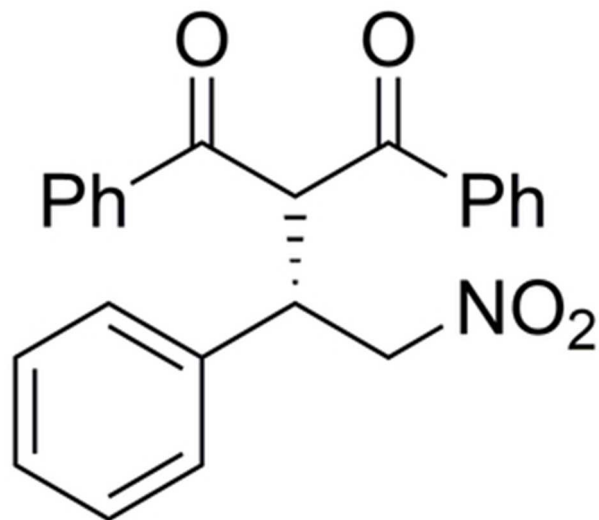
High res (600 dpi) formula 9 for Table 2

29x29mm (300 x 300 DPI)



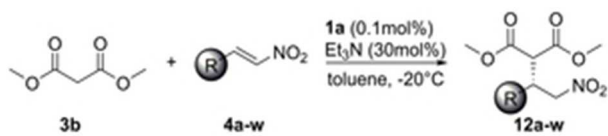
High res (600 dpi) formula10 for Table 2

27x20mm (300 x 300 DPI)



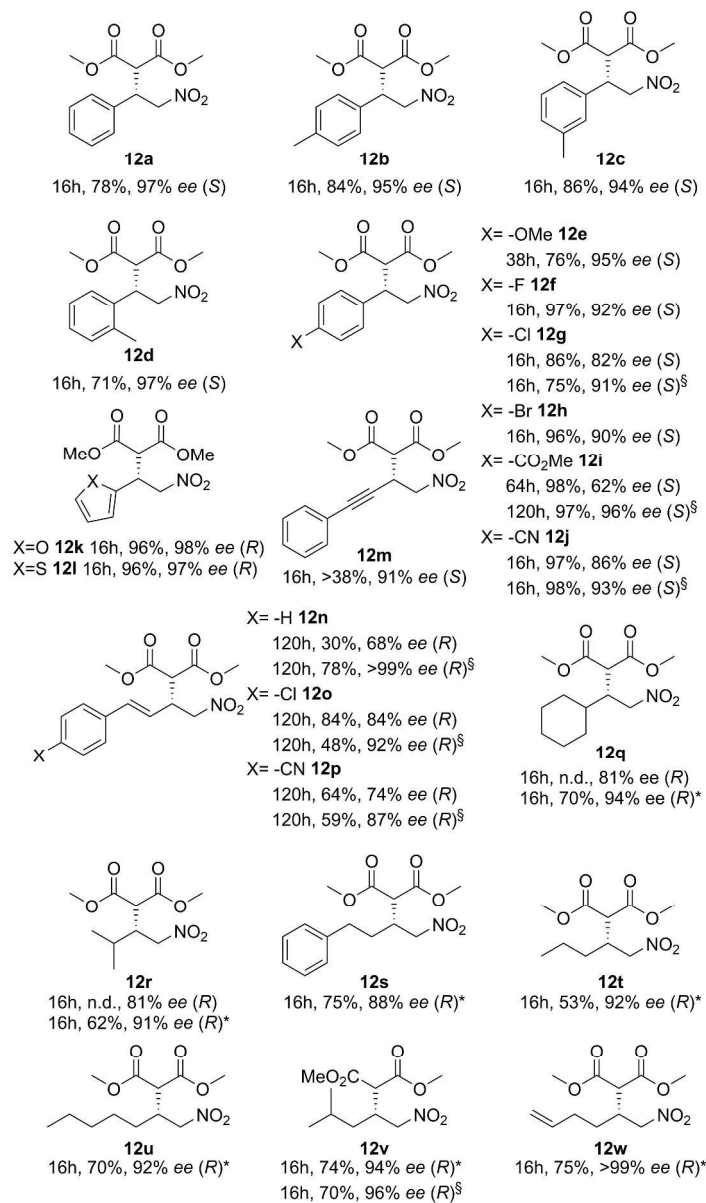
High res (600 dpi) formula 11 for Table 2

25x23mm (300 x 300 DPI)



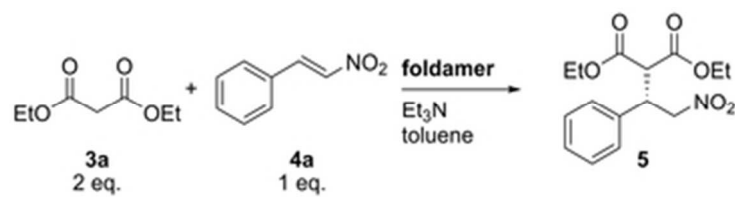
High res (600 dpi) scheme for Table 3

25x5mm (300 x 300 DPI)



High res (600 dpi) scope for Table 3

237x406mm (300 x 300 DPI)



High res (600 dpi) scheme for Table 4

30x8mm (300 x 300 DPI)